

HEAVY VEHICLE STABILITY AND ROLLOVER PREVENTION VIA SWITCHING MODEL PREDICTIVE CONTROL

FITRI YAKUB^{1,2} AND YASUCHIKA MORI²

¹Malaysia-Japan International Institute of Technology
Universiti Teknologi Malaysia
Jalan Semarak, 54100, Kuala Lumpur, Malaysia
mfitri.kl@utm.my

²Graduate School of System Design
Tokyo Metropolitan University
6-6 Asahigaoka, Hino, Tokyo, 191-0065, Japan
ymori@tmu.ac.jp

Received March 2015; revised July 2015

ABSTRACT. *This study contributes to enhancing the maneuverability safety for coordination of active rear steering and direct yaw moment control for un-tripped rollover prevention that makes a panic lane change maneuver to avoid an obstacle in the path. At the same time of avoiding rollover accidents, prohibiting the vehicle from the driver's intended and the vehicle's actual lane, and the effect of crosswind is also important, since it may yield other accidents. Thus, it is necessary to track the driver's desired path as closely as possible while preventing the vehicle from rollover, and maintaining the vehicle stability along the desired path. Here, we start from the results presented by Lee et al., and then, we extend and propose the switching model predictive control which uses direct yaw moment control and active rear steer. Simultaneously, the trade-off between rollover prevention and path tracking is highlighted, and the effectiveness of using switching controllers designed for the trade-off solution is also confirmed through simulation results.*

Keywords: Heavy vehicle, Model predictive control, Vehicle stability, Rollover prevention, Lane change maneuver

1. **Introduction.** Most of the optimal control design approaches rely on dynamic models of the processes to be controlled. Model predictive control (MPC) is a model-based control structure, widely employed for the control of constrained linear or nonlinear systems, including multi-variable systems where a mathematical dynamics process model is used to predict the future behavior of the system, and optimizing the control process performance over a prediction horizon [2,3]. Due to its advantages, MPC has been implemented in several applications particularly related to automotive systems for various active safety and driver assistance systems, vehicle dynamics systems, and autonomous driving and collision avoidance systems, in order to improve vehicle stability, ride comfort, and to prevent traffic accidents [4-6]. Active safety goes further by using loud sounds, visual alerts, and vibrations to direct the driver's attention to imminent danger. These active safety systems are the building blocks for the crash avoiding cars of the future.

Vehicle rollover accidents have been extremely hazardous to the occupants of the vehicle and identified as the most fatal vehicle crashes. According to the Japan Traffic Accidents Databases, rollover accidents were in nearly 1/5 of all the single-vehicle accidents [7]. Because of the high center of gravity, sport utility vehicles, disturbances effect such as gusts of wind, irregular road surfaces, and abrupt maneuver, heavy trucks have a proclivity

to rollover accidents. Thus, it is necessary to develop fast and safety control systems to detect and prevent the rollover, in doing so will enhance vehicle stability.

Rollover prevention and detection such as active braking system (ABS), active suspension, and active stabilizer has been studied extensively in [8-11]. However, installation of dedicated actuators to control active parts is required, increasing the cost which has to be borne by the customer. There are also many control approaches such as active front steering (AFS) [12], active rear steering (ARS) [13], and four-wheel steering [14], which are expected to create a new steering system that exhibits stability and maneuverability in high speed situations during a lane change, create emergency avoidance on a curb or slippery road, degrading the roll rate, and lateral acceleration while going around a bend.

Active front steering has a great influence on lateral vehicle behavior under normal driving situations; however, AFS is no longer able to produce enough lateral force during high acceleration because of highly nonlinear characteristics of the tire. On the other hand, ARS is effective in roll damping and rollover prevention on the low friction surface. While driving under the natural environment such as inclement weather, infrastructure, and topographic features cannot be ignored. ARS can degrade roll motion but it also makes the vehicle deviate from the driver's intended trajectory. Thus, it is necessary to minimize the deviation between the driver's intended trajectory and the vehicle's behavior simultaneously, subject to rollover prevention as a premise.

In this study, we focus on the application of threat avoidance scenario in emergency maneuver control as shown in Figure 1. Such simple threat avoidance without fast safe lane change maneuver and front wheel's reaction as disturbance to the system through MPC has been published and discussed in [15,16]. However, in this paper, we illustrate a scenario where the driver needs to make a safe lane change trajectory due to threats such as a front vehicle making an emergency brake, an animal suddenly appearing, or a divider or kinematic threat. The appearance of these sudden threats forces the controller to react as fast as possible to make a safe lane change before the vehicle crash by taking account of the constraint of the steering angle and the braking torque. Due to the lane change maneuverer, the rollover might happen in fast speed, fast lane change with consideration of the lateral force that might attack the vehicle. Based on these harsh scenarios, the controller is designed to avoid crash from happen.

Thus, we propose MPC controller with switching technique to 1) follow the safe and fast emergency trajectory, 2) prevent the rollover while making lane change, 3) reject the disturbances effect, and 4) enhance the vehicle stability and maneuverability of heavy truck, which is the main novelty in this paper. We compare the performance ability of

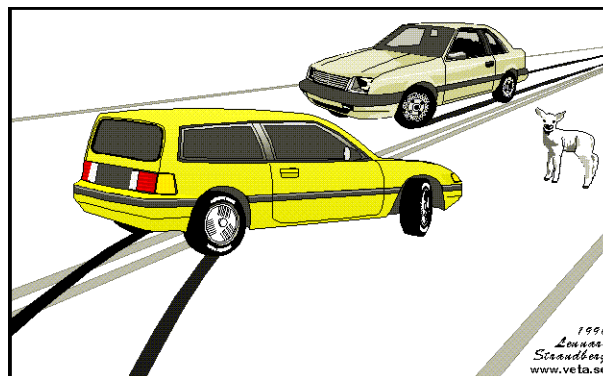


FIGURE 1. Simple example of threat avoidance scenario

the two different controllers in terms of lateral displacement/lane change, yaw rate, and rollover indicator through i) MPC and ii) switching MPC.

As opposed to work in [1] which used a simple MPC design and linear vehicle dynamics model (linear tire model) and neglected the vehicle stability, in this paper, we implemented the controllers to the nonlinear vehicle dynamics model that most represents the real vehicle system. Since the roll dynamics motion will be influenced in high speed conditions, we tested the truck vehicle at middle forward speeds (20 m/s) in a lateral maneuver in a single-lane change scenario.

In this paper, we utilize ABS, which currently focuses on direct yaw moment control (DYC) that produces the corrective yaw moment by using the rear braking forces between the left and the right side of the rear tires, in order to avoid the interferences between AFS and ABS (which become a second contribution of this paper).

This paper is structured as follows. Section 2 describes the full vehicle, nonlinear tire, and disturbance models. Next, the control methods for the linear MPC algorithm and rear braking control concept are explained in Section 3 of obstacle avoidance maneuvers. Furthermore, simulations are performed to validate and examine the proposed method, and the results are discussed in Section 4. Lastly, we conclude and give possible future works in Section 5.

2. System Model. In this paper, we simplify the complexity of the actual vehicle by assuming the front and rear steering angles for both wheels to be the same. We make an assumption that the slip angles at left and right wheels are zero, and the steering angle, the vehicle side slip angle, and the roll angle are approximated to be too small and thus can be neglected. The front and rear suspensions are simplified by equivalent damping and stiffness coefficients. We consider the sprung vehicle mass and the suspension and wheel weights for an un-sprung mass. The pitch motion is neglected. Detailed explanation may be found in [17].

In this paper, we use the following terms: F_x and F_y to denote the longitudinal and lateral tire forces respectively. F_w and M_w represent the force and moment exerted by the side wind respectively, F_z is the normal tire load, and M_z is the total corrective reaction moment from the differential braking; x , y and z correspond to the coordinates of the body frame of a car's position, ω_w is the angular velocity of the tires, v_x and v_y are the longitudinal and lateral wheels velocities respectively, T_b is the wheel torque, δ_f and δ_r express the steering angle of the front and rear wheels, μ is road adhesion coefficient, ψ is the yaw/heading angle and $\dot{\psi}$ is the yaw rate, β is the vehicle side slip angle, and ϕ and $\dot{\theta}$ are the roll and roll rate angle respectively. Some vehicle parameters are explained and given in [17]. The variable at the front and rear wheels is denoted in lower subscripts $(\cdot)_f$ and $(\cdot)_r$.

2.1. Vehicle model. Using the assumptions stated above for the motion longitudinal, lateral, yaw, roll, and rotational dynamics of the front and rear wheels of 8-DoF for the nonlinear model, vehicle motion is described in planar dynamics equations through the following differential equations, as follows:

$$\sum F_x : m(\ddot{x} - \dot{y}\dot{\psi}) = 2F_{xf} + 2F_{xr} - m_s h \dot{\psi} \phi - 2m_s h \dot{\psi} \theta + (l_f - l_r)m_u \dot{\psi}^2 \quad (1)$$

$$\sum F_y : m(\ddot{y} + \dot{x}\dot{\psi}) = 2F_{yf} + 2F_{yr} + m_s h \dot{\theta} - m_s h \dot{\psi} \phi^2 - m_s h \dot{\psi} \theta^2 + (l_r - l_f)m_u \dot{\psi} + F_w \quad (2)$$

$$\begin{aligned} \sum M_z : I_{zz}\dot{\psi} - I_{xz}\dot{\theta} = & t_w/2(-F_{xf,l} + F_{xf,r} - F_{xr,l} + F_{xr,r}) \\ & + 2l_f F_{yf} - 2l_r F_{yr} + (l_r - l_f)m_u(\ddot{y} + \dot{x}\dot{\psi}) + M_w \end{aligned} \quad (3)$$

$$\sum M_x : (I_{xx} + m_s h^2) \dot{\theta} + m_s h (\ddot{y} + \dot{x}\varphi) - I_{xz} \dot{\varphi} = m_s g h \phi - 2k_\phi \phi - 2b_\phi \dot{\phi} \tag{4}$$

$$J_b \dot{\omega}_{wi} = -r_w F_{xi} - T_{bi} - b_w \omega_i, \quad i = (f, r) \tag{5}$$

As tracking the driver’s intended path is also taken into consideration, we defined the inertial trajectory of the vehicle (X, Y) at time t , and from the present position (X_0, Y_0) is described by the following two integral equations:

$$X = X_0 + v_x \int_0^t \cos(\beta + \psi) dt, \quad Y = Y_0 + v_x \int_0^t \sin(\beta + \psi) dt \tag{6}$$

where we choose the initial position (X_0, Y_0) to be zero in all following sections. Since the aims of this paper are for rollover prevention, lane change maneuver, and vehicle yaw stability control, the desired yaw rate must satisfy the upper bound limit as follows:

$$\varphi_{des} \leq \mu g/v_x \tag{7}$$

where the desired yaw rate response cannot always be obtained when tire force goes beyond the adhesion limit of tire, so it has an upper bound limit [18].

2.2. Tire model. The tire dynamics must be considered for the vehicle model, since the tires are the only contact that the vehicle has with the road surface. The existing nonlinear tire model applications and structures that are most frequently used, are determined through the key parameters and analytical considerations based on tire data measurements, that are called the ‘semi-empirical tire model’ or ‘Pacejka tire model’ [19]. Thus, this semi-empirical tire model is adopted in this paper.

The relationship between the longitudinal tire force, the tire slip ratio, and the normal load forces for rear and front wheels because of the weight transfer induced by roll motion and lateral accelerations can be expressed by the following equations:

$$\sqrt{F_{xi}^2 + F_{yi}^2} \leq \mu F_{zi}, \quad i = (f, r) \tag{8}$$

$$F_{zf} = \frac{l_r mg}{2l} - \frac{F_{yf} \phi}{2} - \frac{k_{\phi f} \phi}{t_w} - \frac{b_{\phi f} \dot{\phi}}{t_w} - \frac{h_{uf} F_{yf}}{t_w} - \frac{h_{uf} l_r mg \phi}{t_w l} \tag{9}$$

$$F_{zr} = \frac{l_f mg}{2l} - \frac{F_{yr} \phi}{2} - \frac{k_{\phi r} \phi}{t_w} - \frac{b_{\phi r} \dot{\phi}}{t_w} - \frac{h_{ur} F_{yr}}{t_w} - \frac{h_{ur} l_f mg \phi}{t_w l} \tag{10}$$

where h_{uf} and h_{ur} are the distances of front and rear roll center axis respectively located below the body sprung mass center of gravity.

2.3. Disturbance model. The effect of disturbances on the stability of the vehicle is important, as a bumpy road or irregular road may provide the extra force and torque required to help resist the overturning forces. Here, we assume the front steering angle as a disturbance to the system due to the effect that a driver may drive to abrupt maneuver, and our previous work in [1] reflected that assumption for the front steering angle.

The effect of wind on the stability of the vehicle is important, as a strong gust of wind from the inward or outward side may provide the extra force and torque required to help resist the overturning forces. Here, we neglect the wind effect on longitudinal and roll motion, so according to [20], a side wind impacting the car at the wind velocity as v_w exerts a force and a moment, respectively given by:

$$F_w = \frac{2.5\pi v_w^2}{2}, \quad M_w = \left(\frac{2.5\pi}{2} - 3.3 \left(\frac{\pi}{2} \right)^3 \right) v_w^2 + \frac{(l_f - l_r) F_w}{2} \tag{11}$$

where v_w is the crosswind speeds.

2.4. Rollover indicator. Load Transfer Ratio (LTR) [21], considered to be the most reliable rollover indicator regardless of vehicle configurations and operational conditions, is utilized to detect the onset of the rollover in this paper. The LTR can simply be defined as the load difference between the right and left wheels of the vehicle, normalized by the total load:

$$LTR = \frac{F_{zr} - F_{zl}}{F_{zr} + F_{zl}} \quad (12)$$

where F_{zl} and F_{zr} are defined as the vertical tire forces acting on the left side and right side wheels. The two-wheel lift off of one side of the vehicle occurs if LTR becomes 1 or -1 . We consider LTR to be the threshold of rollover, and establishing LTR is not more than 1 or no less than -1 . We can make a torque balance about the assumed horizontally roll axes in terms of the suspension torques, and the vertical wheel forces by considering un-sprung mass and lateral load transfer due to lateral acceleration:

$$LTR = \frac{2 \left[c\dot{\phi} + k\phi + h_{uf}m_u(\ddot{y} + v_x\varphi - h\dot{\theta})h_u \right]}{mgt_w} \quad (13)$$

where m_u is the vehicle un-sprung mass and h_u is the roll center distance below the sprung mass. The nonlinear vehicle motions in (1)-(13) can be described by the following compact differential equation:

$$\dot{\xi} = f(\xi, u, \omega_d, r_{des}), \quad \eta = h(\xi) \quad (14)$$

where the state, input, disturbance, reference, and output vectors are given as:

$$\begin{aligned} \xi &= [v_y \ Y \ X \ \varphi \ \psi \ \theta \ \phi \ \omega_f \ \omega_r \ LTR]^T, \quad u = [\delta_r \ M_z]^T, \\ \omega_d &= [\delta_f \ F_{wy} \ M_{wz}]^T, \quad r_{des} = [Y_{des} \ \psi_{des}]^T, \quad h(\xi) = [Y \ \psi]^T \end{aligned} \quad (15)$$

3. Integrated Control Method. The block diagram of the controller design of switching MPC is illustrated in Figure 2. Figure 2 illustrates the control structure for ARS that uses rear steering, active braking system that uses the reaction moment at front and rear wheels (DYC) as a control input to the system. These control inputs are used to control the vehicle in order to avoid the avoidance, prevent the rollover, and be able to make a safe lane change maneuver by following a given reference trajectory, while enhancing vehicle yaw stability. It comprises a constant vehicle speed, safety reference trajectory, the controllers (MPC/switching MPC), vehicle model with nonlinear tire model, and the crosswind effect as disturbance to the system. MPC will be implemented in the same way of switching MPC in order to compare fairly.

3.1. Linear MPC. Model predictive control was designed based on 3-DoF yaw-roll motion by linearizing the equations from the vehicle and tire model:

$$\begin{aligned} m\dot{v}_y &= \frac{1}{I_{xx}v_x} \left[-(C_r + C_f)J_{xq}v_y + ((C_rl_r - C_fl_f)J_{xq} - I_{xx}mv_x^2) \varphi \right] \\ &\quad - \frac{1}{I_{xx}} [m(hb_\phi)\theta - mh(mgh - k_\phi)\phi - C_fJ_{xq}\delta_f + C_rJ_{xq}\delta_r] \end{aligned} \quad (16)$$

$$I_{zz}\dot{\varphi} = \frac{1}{v_x} [(C_rl_r - C_fl_f)v_y - (C_fl_f^2 + C_rl_r^2)\varphi] + C_fl_f\delta_f - C_rl_r\delta_r - \frac{t_w p_i}{2} \quad (17)$$

$$I_{xx}\dot{\theta} = \frac{h}{v_x} [(C_rl_r - C_fl_f)\varphi - (C_f + C_r)v_y] - b_\phi\theta + (mgh - k_\phi)\phi + C_fh\delta_f + C_rh\delta_r \quad (18)$$

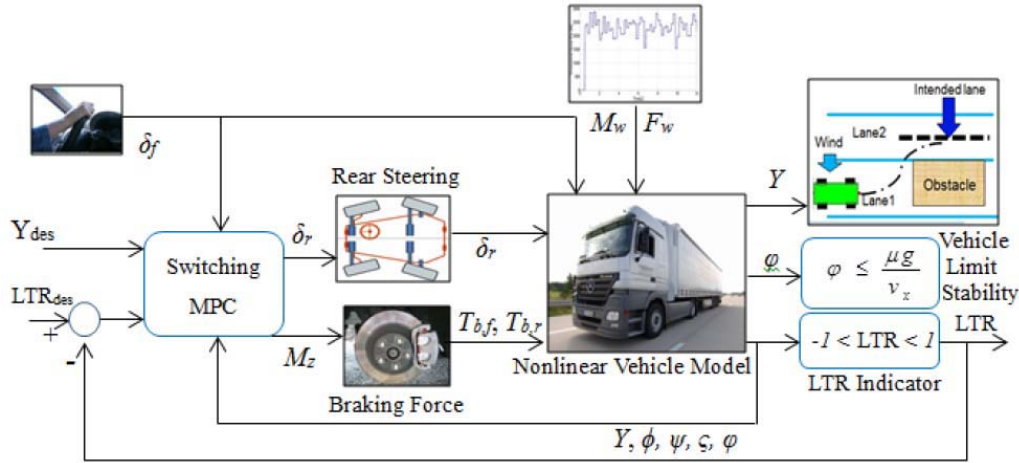


FIGURE 2. Model predictive control via active rear steering with active braking system

For a DYC that produces the reaction moment which happens at the front and rear wheels due to the steer angle effect that function as an external yaw moments (M_z) can be described by the following equivalent equations:

$$M_f \approx 2l_f C_f M_z, \quad M_r \approx 2l_r C_r M_z \tag{19}$$

The vehicle motions in (16)-(18) can be represented in a given state-space structure with $\dot{x} = [\dot{v}_y \ \dot{\phi} \ \dot{\theta}]^T$ as:

$$\dot{x} = Ax + B_1 u + B_2 \omega_d + B_3 r_{des}, \quad y = Cx + Du \tag{20}$$

As the MPC is designed based on a mathematical model of the plant in discrete time, we discretize the vehicle dynamics in (20) by neglecting an unmeasured disturbance to obtain:

$$x_l(k+1|k) = A_l x_l(k|k) + B_l u_l(k|k) + B_2 \omega_{dl}(k|k), \quad y_l(k|k) = C_l x_l(k|k) + D_l u_l(k|k) \tag{21}$$

where $x_l(k|k)$ is the state vector at time step k , and $x_l(k+1|k)$ is the state vector at time step $k+1$, with $x_l(k|k) \in R^{x(k|k)}$, $u_l(k|k) \in R^{u(k|k)}$, $\omega_{dl}(k|k) \in R^{\omega_d(k|k)}$, and $y_l(k|k) \in R^{y(k|k)}$ representing the state, control input, measured disturbance, and measured output vectors respectively. We define:

$$x_l(k) = [v_y \ Y \ \varphi \ \psi \ \theta \ \phi]^T, \quad u_l(k) = [\delta_r \ M_z]^T, \quad \omega_{dl}(k) = [\delta_f], \quad y_l(k) = [Y \ \psi]^T \tag{22}$$

Because of the understeer effect of the differential braking force, it is impossible to follow the driver's desired trajectory accurately. However, the vehicle is asked to track the driver's desired Y -axis placement during a lane change maneuver in simulations.

The objective of the predictive control system is to find the optimal control input vector $\Delta \tilde{u}_l(k+i|k)$ such that an error function between the predicted output and the reference signal is minimized. The optimization of the predictive control system will be solved by minimizing the cost function, and given by:

$$\text{Minimize : } J_{mpc}(k) = \sum_{i=1}^{H_p} \|\tilde{y}_l(k+i|k) - r_{des}(k+i|k)\|_{S_q(i)}^2 + \sum_{i=0}^{H_c-1} \|\Delta \tilde{u}_l(k+i|k)\|_{S_r(i)}^2 \tag{23}$$

where the first summation of the cost function refers to the minimization of trajectory tracking errors between the predicted outputs $\tilde{y}_l(k+i|k)$, ($i = 0, \dots, H_p - 1$) and the

output reference signals $r_{des}(k + i|k)$, ($i = 0, \dots, H_p - 1$). The second summation in (23) penalizes the control signal effort of the rear steering angle $\Delta\tilde{u}_l(k + i|k)$, ($i = 0, \dots, H_c - 1$) of the active rear steering control maneuver. Here, $r_{des}(k + i|k)$ consists of the reference value of lateral position and yaw angle.

We formulate the optimization of the predictive control system through cost function in (23), which takes the constraints of an actuator into consideration, which is written as:

$$\begin{aligned}
 & \min_{\Delta U_k} J(x_l(k), \Delta U_{lk}) \\
 & \text{subject to :} \\
 & \hat{x}_l(k + 1|k) = A_l x_l(k|k) + B_l u_l(k|k) + B_2 \omega_{dl}(k|k) \\
 & \hat{x}_l(k + 2|k) = A_l \hat{x}_l(k + 1|k) + B_l \hat{u}_l(k|k) + B_2 \hat{\omega}_{dl}(k|k) \\
 & \quad \vdots \\
 & \hat{x}_l(k + i|k) = A_l \hat{x}_l(k + i - 1|k) + B_l \hat{u}_l(k + i - 1|k) + B_2 \hat{\omega}_{dl}(k + i - 1|k) \quad (24) \\
 & \delta_{r,\min} \leq \hat{u}_{1l}(k + i|k) \leq \delta_{r,\max} \\
 & \Delta\delta_{r,\min} \leq \Delta\hat{u}_{1l}(k + i|k) \leq \Delta\delta_{r,\max} \\
 & M_{z,\min} \leq \hat{u}_{2l}(k + i|k) \leq M_{z,\max} \\
 & \Delta M_{z,\min} \leq \Delta\hat{u}_{2l}(k + i|k) \leq \Delta M_{z,\max} \\
 & Y_{\min} \leq \hat{y}_{1l}(k + i|k) \leq Y_{\max} \\
 & \psi_{\min} \leq \hat{y}_{2l}(k + i|k) \leq \psi_{\max}, \quad i = 1, \dots, H_p
 \end{aligned}$$

The variation in the rear steering angle $\Delta\tilde{u}_l(k + i|k)$ can be obtained when the cost function is made to be as small as possible. The weight matrixes $S_q(i)$ and $S_r(i)$ are semi-positive definite and positive definite respectively, which can be adjusted for the desired closed-loop performance. We defined $S_q(i)$ as state tracking weight because the error $\tilde{y}_l(k + i|k) - r_{des}(k + i|k)$ can be made as small as possible by enlarging $S_q(i)$. Similarly, $S_r(i)$ is defined as the input tracking weight and the variation of input is reduced to make the response of the system slow by enlarging $S_r(i)$. The predictive and control horizon is usually assumed to be $H_p \geq H_c$ and the control signal is assumed constant for all $H_c \leq i \leq H_p$.

Then, an optimal input was calculated for the next *time* step instead of being calculated for the immediate *time* step by solving convex optimization problems at every *time* steps.

3.2. Braking control allocation. In this section, the desired direct yaw moment control M_z is adopted from the differences between the two sides of the vehicle torque as denoted in (5) [22]. In our study, the braking torque is activated only according to the yaw rate; i.e., only used when the vehicle goes towards instability or emergency maneuvers because of its direct effects on the longitudinal motion, while the rear steering angle is considered for the entire maneuver to be in control or in normal driving maneuvers. This means we consider two control inputs: rear steering angle, and differential braking at rear left and right tire, but only a single control input is activated at one time.

The control law is designed to select the most effective wheels to apply the brake torque, which depends on the steering condition. Oversteering happens when the vehicle yaw rate is larger than the desired yaw rate, so the outer wheels will be selected to generate a counter-cornering yaw moment. Understeering happens when the vehicle yaw rate is smaller than the desired yaw rate, so the inner wheels will be chosen to generate a pro-cornering yaw moment.

In this study, we only used one wheel at a time to generate the controlled moment because the vehicle is not as much decelerated as when brake torque is applied at more than one wheel to generate the same amount of yaw moment. Since front steering angle command is activated as the driver abruptly maneuvers the disturbance, only rear wheels

are involved in the control law:

$$T_{b,rl} = \frac{2M_z r_w}{t_w}, \quad T_{b,rr} = \frac{-2M_z r_w}{t_w}, \quad e_\psi < 0, \quad \varphi > 0 \quad (25)$$

$$T_{b,rl} = \frac{2M_z r_w}{t_w}, \quad T_{b,rr} = \frac{-2M_z r_w}{t_w}, \quad e_\psi > 0, \quad \varphi < 0 \quad (26)$$

3.3. Switching technique. The switch control law presented aims to activate ARS to track the driver's intended lane by means of active rear wheel steer. Control of DYC is flipped to ARS under lateral position-based switching control, when the trajectory overpasses the intended path. Here, the switching signal of the two controllers is set based on lateral position limit and can be described as:

$$T_{b,rl} = \begin{cases} \text{DYC off } (0 < Y \leq 10 \text{ m}) \\ \text{DYC on } (Y > 10 \text{ m}) \end{cases} \quad (27)$$

Under the rear steering control in ARS maneuver, the vehicle does not roll over because rear steer angle controlled is strictly constrained. Same goes to DYC maneuver control where the brake torques of the rear tires are also limited by the constrained. The input and input rate constraints of rear steer angle and brake torques of DYC are set as follows:

$$-0.5 \text{ rad} \leq \delta_r \leq 0.5 \text{ rad}, \quad -0.4 \text{ rad/s} \leq \Delta\delta_r \leq 0.4 \text{ rad/s} \quad (28)$$

$$\begin{aligned} -1500 \text{ Nm} &\leq M_z \leq 1500 \text{ Nm}, \\ -1000 \text{ Nm/s} &\leq \Delta M_z \leq 1000 \text{ Nm/s} \end{aligned} \quad (29)$$

If output weight matrix $S_q(i)$ is enlarged, the vehicle can be controlled to converge to the reference lane trajectory immediately. On the other hand, if input weight matrix $S_r(i)$ is enlarged, the variation of rear wheel steer is restrained and the convergence will be slowed.

In the case of the measured yaw angle exceeds the threshold value as stated in (25) and (26), the switching signal control will be turned on and the braking force is controlled to revise yaw moment. As the response delay of MPC is taken into consideration, we set the threshold value to 0.4 radian which is smaller than the constraint of yaw angle presented. The constraints of Y -axis placement and yaw angle are set as follows:

$$-0.4 \text{ rad} \leq \psi \leq 0.4 \text{ rad}, \quad 0 \leq Y \leq 10 \text{ m} \quad (30)$$

4. Simulation and Discussion. The proposed methods' controllers are implemented for a vehicle path following on a single-lane change or threat avoidance scenario.

4.1. Scenario description. The vehicle is considered to be travelling horizontally, following the path with a $v_x = 20$ m/s without braking or accelerating. The typical obstacle avoidance maneuver is simulated with a peak driver steering input of magnitude to be at 100° , so δ_f under the initial driving conditions is assumed to act in the direction of the path at $t = 2$ s acting as a measurable disturbance on the vehicle.

This disturbance represents the shock reaction or over control from the driver when the threat suddenly appears. It might also be that the driver did not really concentrate on the car, i.e., staring at mobile phone, reading a new e-mail message, texting a friend, or other activities instead of looking at the road or the car in front. According to the NHTSA, driver distraction is a factor in almost 20 percent of crashes in which someone is injured. This situation is a common occurrence, so the controller is needed to counterattack the problem caused by the driver. The δ_f disturbance is shown in Figure 4.

The second disturbance is the drag force and torque given in (11) under the initial driving conditions is assumed to act in the direction of the path at $t = 1$ s with $v_w = 10$ m/s, acting as an unmeasured disturbance on the vehicle. The forces and torques arising

from this sidewise-acting wind gust are assumed to be persistent and are applied as step functions throughout the simulation time. Simulations were performed by using the Model Predictive Control Toolbox in Matlab and Simulink software within 15 seconds.

In this study, the predictive controllers were carried out through reducing the vehicle deflection from the preferred path to attain the main goal which is to avoid emergency avoidance by following the given trajectory indicated as safe lane change trajectory as close as possible. Both controllers have been designed based on linear 3-DoF vehicle motion to the nonlinear vehicle system at middle (20 m/s) forward speed. In this scenario, we compared the performance of the controller design for rollover prevention, lateral position, and yaw stability control to both without the controller and with proposed method. Here, we set the single-lane change maneuver at 10 degree step input representing a 10 meter starting from $t = 0.5$ s or $Y_{ref} = 10$ m, $\psi_{ref} = 0$ as shown in Figure 4. The yaw stability limit must satisfy the stability criteria of Equation (2) given approximated $\varphi \leq \mu g/v_x \approx 0.49$ rad/s.

Table 1 lists the MPC parameters with weighting matrices that were designed and implemented in ARS with the DYC maneuver scenarios for both scenarios with and without the switching method. The weighting matrices for input and outputs of MPC are selected based on trial and error from the best output responses, where, first we need to tune the gain of MPC under ARS, and then tune MPC under DYC maneuver later until we satisfy the result performances.

TABLE 1. Controller parameters condition

Parameter	MPC	Switching MPC
H_p, H_c	20, 9	20, 9
Sampling time, T_s [s]	0.05	0.05
δ_f [deg], $\Delta\delta_f$ [deg/s]	$\pm 30, \pm 20$	$\pm 30, \pm 20$
$R_1, R_2, \Delta R_1, \Delta R_2$	0.9, 0.02, 0.3, 0.03	0.1, 0.1, 0.03, 0.03
Q_{11}, Q_{22} ($v_x = 20$ m/s)	0.035, 0.155	0.021, 0.151

4.2. Result and discussion. Prior to proposed simulations, we carried out standard vehicle maneuvers tests to validate our model in the open-loop simulation scenario. In this paper, we performed only the Double-Lane Change test, for the purpose of testing improvement to existing vehicle and for vehicle validation purposes in the open-loop simulation, as displayed in Figure 3. The vehicle speed was set at 20 m/s, which is suitable for the test, with a road surface coefficient of 1. As illustrated in Figure 3, the vehicle response in terms of roll angle, roll rate, yaw rate, and lateral acceleration due to steer angle has been proven to be validated, thus suitable for other simulations.

The first simulation revolves around the vehicle motion responses at a constant forward speed of 20 m/s on a single-lane change scenario without the controller to the system as shown in Figure 4. It can be seen clearly that without the controller, the single-lane change maneuver failed to follow the trajectory as decided at 10 m, leading to the collision. The response of LTR motion indicates that the vehicle is not stable where one side of the tire is not attached to the ground while trajectory is going on as shown through its steady-state position. Simulation results also showed that the yaw stability for the vehicle is worse after 5 seconds and becomes more unstable after surpassing the limit of the stability. Moreover, we can analyze the lateral acceleration that demonstrates that the vehicle is not stable when it shows the acceleration is infinite after 5 seconds. Figure 4 illustrates that the vehicle requires the controller to improve the vehicle's response by stabilizing the maneuverability in order to avoid any car crash accident.

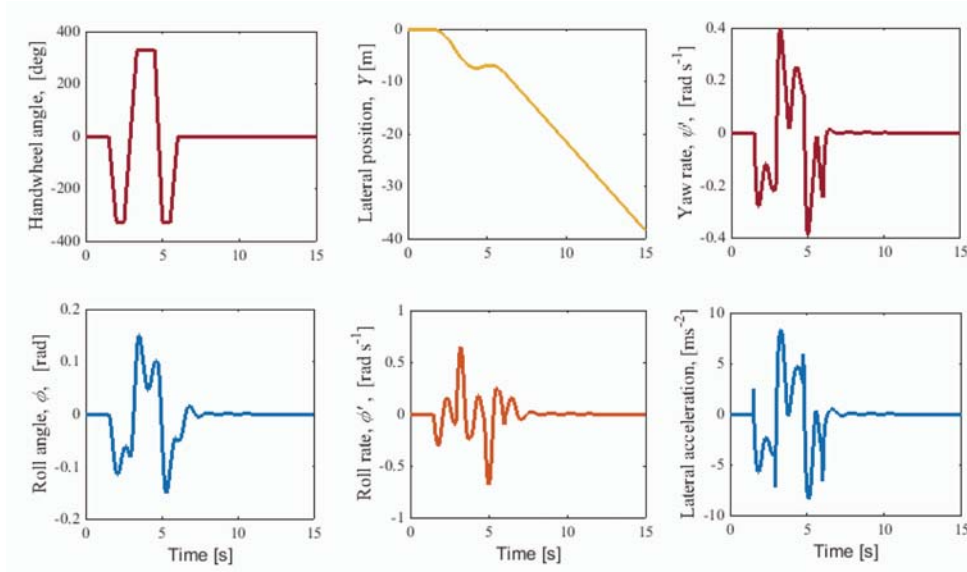


FIGURE 3. Vehicle maneuver test of double-lane change at 20 m/s with $\mu = 1$

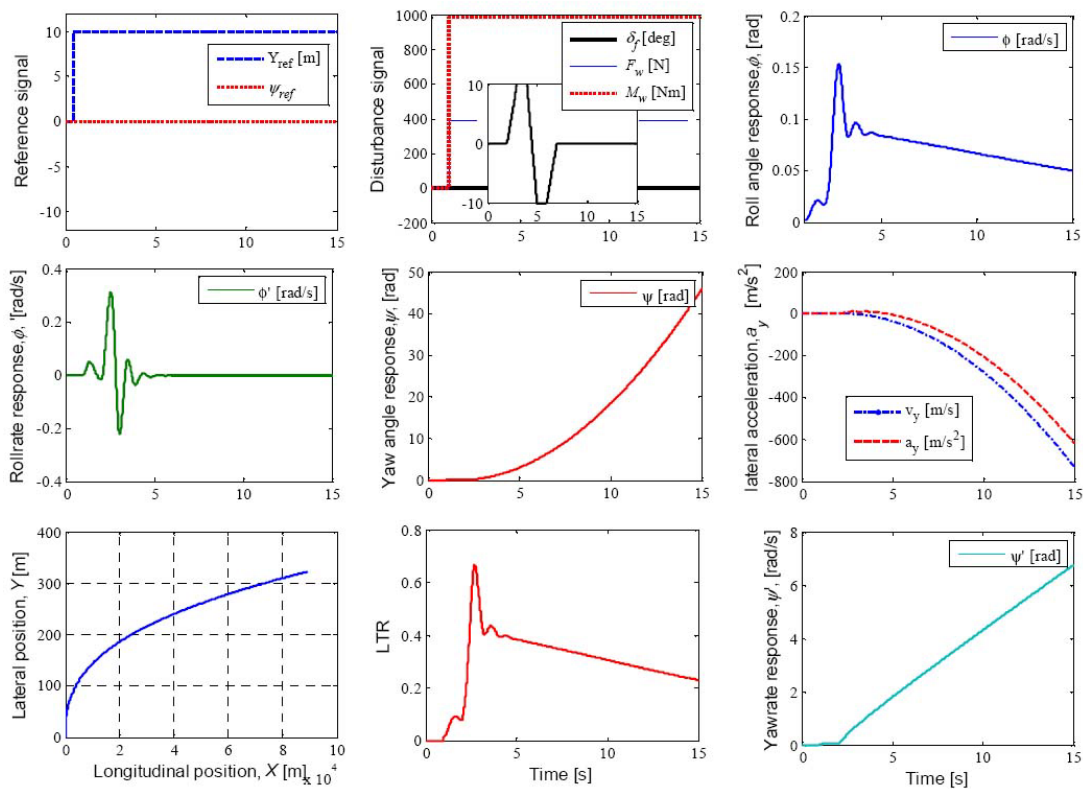


FIGURE 4. Vehicle performances without controller

In the second simulation process, we employed MPC only and compared the results of the vehicle motion responses for the lateral displacement, vehicle heading angle, load transfer ratio, and lateral acceleration to an ARS maneuver, as demonstrated in Figure 5. From Figure 5, it can be clearly seen that for ARS maneuver, trajectory tracking responses of threat avoidance for lateral displacement were worse especially under disturbances effects. It shows that under ARS maneuver control, the lateral position oscillates a few time before it achieves the desired path.

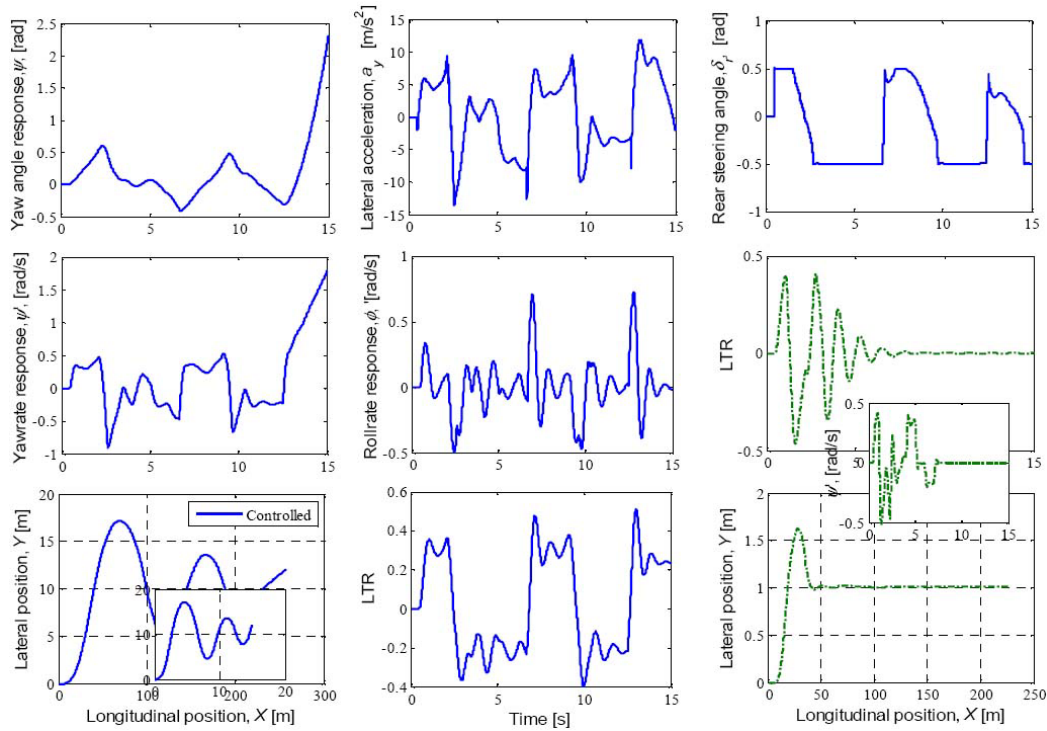


FIGURE 5. Vehicle performances with active rear steering maneuver control

For the yaw rate response, ARS maneuver is not able to maintain the vehicle stability at steady-state conditions where the vehicle response becomes unstable and spin after 12 seconds. Same goes for the LTR and lateral acceleration responses for ARS maneuver control, where LTR responses indicate that the vehicle is not stable due to both tire not being attached to the ground, but a rollover does not occur. Since ARS only depends on rear steer wheel as a control variable which showed it saturated at ± 0.5 rad, it is impossible to control multivariable outputs.

Moreover, we would like to investigate the effectiveness of the ARS maneuver control, so the results in Figure 5 showed that the ARS maneuver control performed well when the lateral position reference is set to 1 m; it gave yaw stability response within the range, and LTR response also performed better; the vehicle was stable and tires were attached to the ground. However, 1 m is not a practical range to make a lane change maneuver or avoiding an obstacle since this distance will still make the car crash with the obstacle.

Next, we would like to investigate the effectiveness of proposed switching MPC method compared to MPC under the disturbances. Since previous discussions described that ARS maneuver control is not effective in controlling the vehicle stability and rollover, here, we would only discuss the ARS with DYC maneuver for switching MPC and MPC control. Based on the same scenario, we simulated the heavy vehicle with the same speed at 20 m/s for both controllers as shown in Figure 6. Figure 6 indicates that both controllers behaved and acted very well for lateral position and yaw angle even under disturbances effect. However, if we scrutinize in lateral position responses, we might find that the switching MPC controller can decrease the undershoot from 15% to 8%, which indicates more accurate and safe lane changes compared to MPC. However, both controllers need at least 3 to 3.5 seconds to make a safe change lane from their initial condition at 0.5 seconds before the vehicle hits the threat. From the lateral responses, we noticed that switching MPC to achieve the target trajectory is faster compared to MPC.

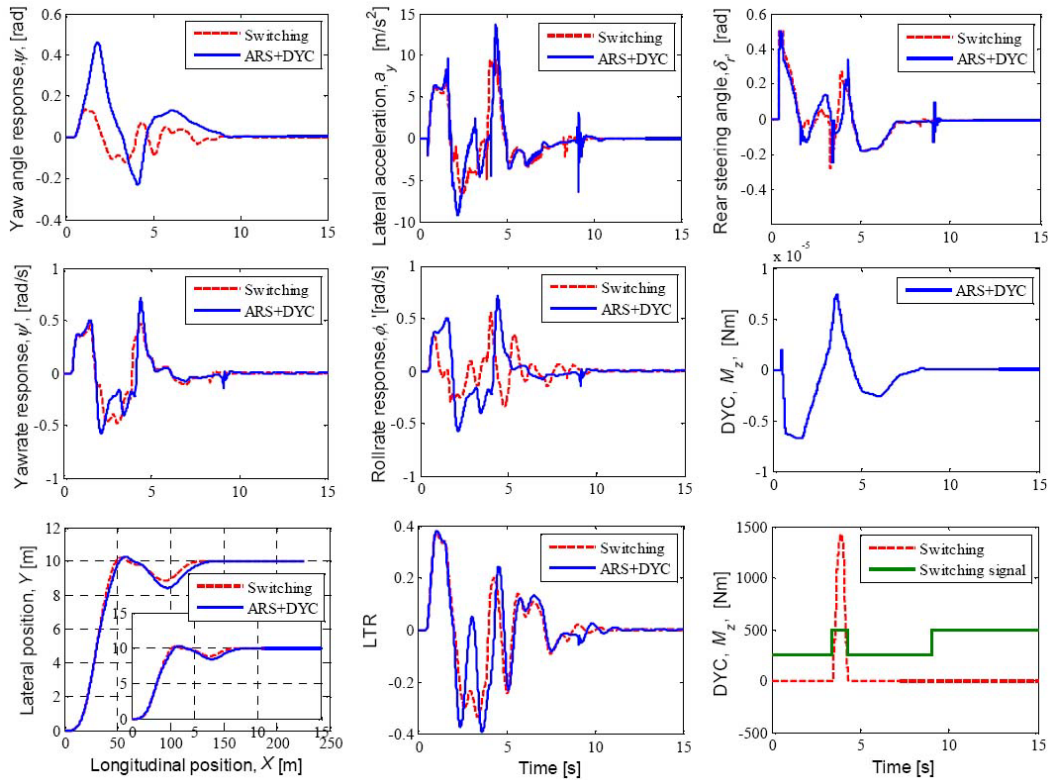


FIGURE 6. Vehicle performances with switching predictive control of active rear steering and direct yaw moment maneuver control

On the other hand, for the yaw rate response, the switching MPC is able to maintain the vehicle stability below the stability limit (less than 0.5 rad/s) compared to the MPC and manages to achieve steady-state condition. For the MPC, the yaw rate response goes over the limit at 4.5 seconds, indicating that the vehicle is not in a stable position. This implies that DYC is highly influential in controlling the lane change maneuver at reference through switching technique rather than the combination of both input variable as described in switching signal response. From the switching signal, we noticed that when the lateral response goes over the limit of 10 m, then the switching MPC starts to switch the control variable from the rear steering to DYC. It shows that DYC in switching MPC method is only used when it is really needed and both control variables are not responding at the same time (opposite to MPC, where both control variables are used through all simulation processes).

Moreover, for the LTR responses, it can be clearly seen that both methods performed very well, which demonstrates that both sides of the wheels are touching the ground, and no rollover occurred during the maneuver under the disturbance. The LTR response is not much different between both controllers; however, switching MPC method achieves the steady state condition and less oscillation earlier compared to MPC. It proved that both controllers perform well in preventing the rollover from happening. Figure 5 also shows that the lateral acceleration for both control methods are stable, where the steady state of the acceleration is at zero. However, it can see from the lateral acceleration responses that switching MPC is less than MPC where, particularly, around 4.5 seconds MPC response is high speed, which influences the vehicle to surpass the vehicle stability limit.

Furthermore, from the control signal responses, the rear steering angle was constrained for both controllers particularly at 0.5 seconds when the vehicle is forced to make a lane

change from 0 to 10 m. For MPC controller, where at this time, the braking control takes over the control of the vehicle and for switching MPC, the rear steering still used to control the vehicle. For ARS and DYC maneuver, this indicates the advantages of the MPC approach that can be implemented in multivariable system, also for constraints taken into account.

5. Conclusions. The paper presents an integrated controlled approach for an ARS and ABS maneuver of heavy vehicle in a path following control considering the front wheel steering and gust of wind as disturbances at middle forward speed on a single-lane change or obstacle avoidance scenario. An ARS that utilizes the rear steering command and an ABS that utilizes the differential rear braking are designed based on switching MPC through a simple 3-DoF vehicle model with linear tire approximations. The simulation results proved that the right and left wheel brake distribution that provided the ABS was more effective and successfully implemented with a combination of ARS for vehicle steering maneuvers even under a disturbance effect to the lateral and yaw motions. The improvement of the control methods with different combinations such as active roll, active suspension, and braking with front and rear wheels may be considered and left for further work. The proposed method is suggested to be implemented in real applications soon.

Acknowledgment. The authors would like to thank Mr. Shihao Lee for imparting such good knowledge related to this research. Special thanks is also extended to Dr. Ahmad Zahran M. Khudzari for his help preparing this manuscript.

REFERENCES

- [1] S. Lee, F. Yakub, M. Kasahara and Y. Mori, Rollover prevention with predictive control of differential braking and rear wheel steering, *Proc. of the 6th Int. Conf. Robotics, Automation and Mechatronics*, Manila, Philippines, pp.144-149, 2013.
- [2] S. J. Qin and T. A. Badgewell, An overview of industrial model predictive control technology, *Chemical Process Control*, vol.93, pp.232-256, 1997.
- [3] Y. Xia, G. Liu, P. Shi, J. Chen and D. Rees, Robust constrained model predictive control based on parameter-dependent Lyapunov functions, *Circuit System and Signal Processing*, vol.27, no.4, pp.429-446, 2008.
- [4] L. D. Baskar, B. De Schutter and H. Hellendoorn, Optimal routing for automated highway systems, *Transportation Research Part C: Emerging Technologies*, vol.30, pp.1-22, 2013.
- [5] J. Nilsson and J. Sjöberg, Strategic decision making for automated driving on two-lane, one way roads using model predictive control, *Proc. of IEEE Intelligent Vehicles Symposium*, Gold Coast, pp.1253-1258, 2013.
- [6] F. Yakub and Y. Mori, Comparative study of autonomous path-following vehicle control via model predictive control and linear quadratic control, *J. of Automobile Engineering*, doi no: 10.1177/0954407014566031, 2015.
- [7] http://www.itarda.or.jp/english/e_outline1.php.
- [8] S. F. van der Westhuizen and P. S. Els, Slow active suspension control for rollover prevention, *J. of Terramechanics*, vol.50, no.1, pp.29-36, 2013.
- [9] H. Mirzaeinejad and M. Mirzaei, Optimization of nonlinear control strategy for anti-lock braking system with improvement of vehicle directional stability on split- μ roads, *Trans. Research Part C*, vol.46, pp.1-15, 2014.
- [10] P. Safi and M. M. Entezari, Fuzzy controller design for a novel vehicle rollover prevention, *Int. J. of Machine Learning and Computing*, vol.2, no.5, pp.1-4, 2012.
- [11] R. Tchamna, E. Youn and I. Youn, Combined control effects of brake and active suspension control on the global safety of a full-car nonlinear model, *Vehicle System Dynamics*, vol.52, pp.69-91, 2014.
- [12] J. Yoon, W. Cho, J. Kang, B. Koo and K. Yi, Design and evaluation of a unied chassis control system for rollover prevention and vehicle stability improvement on a virtual test track, *Control Eng. Practice*, vol.18, no.6, pp.585-597, 2010.

- [13] M. Doumiati, O. Sename, L. Dugard, J. M. Martinez-Molina, P. Gaspar and Z. Szabo, Integrated vehicle dynamics control via coordination of active front steering and rear braking, *European J. of Control*, vol.19, pp.121-143, 2013.
- [14] A. Tavasoli, M. Naraghi and H. Shakeri, Optimized coordination of brakes and active steering for a 4WS passenger car, *ISA Trans.*, vol.51, no.5, pp.573-583, 2012.
- [15] N. J. L. Noxon, *A Model Predictive Control Approach to Roll Stability of a Scaled Crash Avoidance Vehicle*, Master Thesis, California Polytechnic State University, 2012.
- [16] J. Shin, J. Huh and Y. Park, Asymptotically stable path following for lateral motion of an unmanned ground vehicle, *Control Eng., Practice*, vol.40, pp.102-112, 2015.
- [17] F. Yakub and Y. Mori, Enhancing path following control performance of autonomous ground vehicle through coordinated approach under disturbance effect, *IEEJ Trans. on Electronics, Information and Systems*, vol.125, no.1, 2015.
- [18] E. J. Bedner and W. G. Chester, Methods, systems, and computer program products for tire slip angle limiting in a steering control system, *U.S. Patent No. 7,756,620*, 2010.
- [19] H. B. Pacejka, *Tire and Vehicle Dynamics*, 3rd Edition, Elsevier Ltd, Oxford, 2012.
- [20] T. Keviczky, P. Falcone, F. Borrelli, J. Asgari and D. Hrovat, Predictive control approach to autonomous vehicle steering, *Proc. of Amer. Cont. Conf.*, MN, US, pp.4670-4675, 2006.
- [21] C. Larish, D. Piyabongkarn, V. Tsourapas and R. Rajamani, A new predictive lateral road transfer ratio for rollover prevention systems, *IEEE Vehicular Technology*, vol.62, no.7, pp.2928-2936, 2013.
- [22] T. Shim, D. Toomey, C. Ghike and H. M. Sardar, Vehicle rollover recovery using active steering/wheel torque control, *Int. J. Vehicle Design*, vol.46, no.1, pp.51-71, 2008.